

Polyelectrolyte–Gelatin Complexation: Light-Scattering Study

W. A. Bowman, M. Rubinstein,*† and J. S. Tan*

Imaging Research and Advanced Development, Eastman Kodak Company, Rochester, New York 14650-2116

Received December 27, 1996; Revised Manuscript Received March 31, 1997

ABSTRACT: Complex formation between negatively charged polyelectrolytes and a net negatively charged polyampholyte (gelatin) has been characterized by light scattering. The two polyanions studied are sodium poly(styrenesulfonate) (NaPSS) and sodium poly(2-acrylamido-2-methylpropanesulfonate) (NaPAMS). The molecular weights of the single polyelectrolyte chains NaPSS and NaPAMS increase 20- and 15-fold, respectively, upon saturation with gelatin. Despite such molecular weight increases, the radii of gyration of the complexes were found to be only slightly larger (~15%) than those of the corresponding parent polyelectrolytes. Increasing negative values for the second virial coefficients were observed upon saturation of gelatin on the polyanion chains, indicating increasing interchain attraction. Both the stoichiometries and sizes of the complexes decrease monotonically with pH. At a constant pH, the complex stoichiometry peaks around 0.01 N NaAc. These results suggest that electrostatic interaction is the main driving force for complexation in these systems. Polyampholyte molecules are polarized in the electric field of a polyelectrolyte chain. This polarization-induced attraction is believed to be the main mechanism of complexation. Charge density of the polyanion is suggested to be an important factor for determining its extent of gelatin binding.

I. Introduction

Polymer–polymer complexes can be formed as a result of interchain interaction when two macromolecules are mixed in solution.^{1–4} The association may be driven by Coulombic attraction or other interactions, such as hydrogen bonding, dipole–dipole interaction, charge-transfer interaction, and the hydrophobic effects. These forces are important factors in determining the overall configuration and stability of the complexes. The resulting complexes may remain in solution, may phase separate into coacervate liquids, or may precipitate as amorphous solids or a gel, depending on the concentrations, the mixing conditions, and the structures of the parent polymers. Practical applications of such phenomena include: (1) microencapsulation of water-insoluble molecules, such as pigments, drugs, or proteins,^{5,6} (2) protein separation and purification,⁷ (3) models for understanding protein–nucleic acid interactions in cells, and cell transformation⁸ or gene therapy,⁹ and (4) thickening agents for coating fluids in photographic and food¹⁰ industries.

Recent efforts on dilute solution characterization studies of polyelectrolyte complexation have been focused mostly on two linear, oppositely charged, synthetic homopolymers^{1,11–13} or copolymers.^{14,15} In general, precipitation occurs when the molar ratio of the two oppositely charged groups reaches unity, resulting in electroneutrality. The displacement of counterions initially associated with a given polyion by an oppositely charged long-chain polyion is related to cooperative interaction between the two polyelectrolyte chains. The reduced solubility of the resulting complex in water is attributed to dehydration or increase in hydrophobicity upon salt formation. Nonstoichiometric composition of the two polymers, however, was shown to produce water-soluble complexes when one chain is much longer than the other.^{11,12}

Studies on the interactions between polyelectrolytes and globular proteins bearing a net charge of the

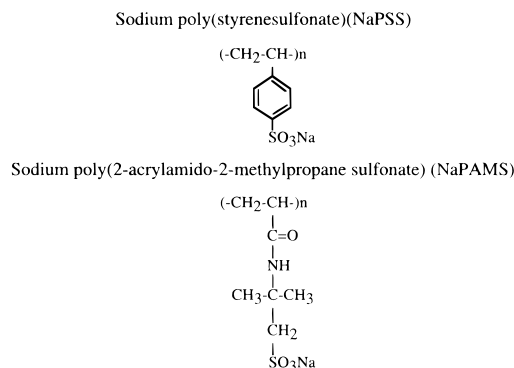


Figure 1. Chemical structures for the sulfonate-containing polyelectrolytes.

opposite sign as that of the polyelectrolytes have also been reported by several workers.^{11,16–22} The driving forces for association similar to those for the oppositely charged linear chains should also be operative. However, the mechanism of interaction between polyion and ampholytic protein with a net charge of the same sign as that of the polyion is less understood. Few examples of the latter system include polyanions with bovine serum albumin at pH > pI_{iso} (with a net negative charge)^{16,17,21} and a polycation with lysozyme at pH < pI_{iso} (with a net positive charge),²⁰ where pI_{iso} is the isoelectric point of the protein. In such cases, the presence of nonuniform “surface charge patches” on the globular proteins^{16,17} is believed to be important for complexation.

Instead of two linear oppositely charged polyelectrolytes or globular proteins and polyelectrolytes, we are interested here in the interaction between a flexible ampholytic gelatin chain molecule (alkali-processed, type IV, pI_{iso} = 4.9) and negatively charged linear polyanions, such as sodium poly(styrenesulfonate) (NaPSS) or sodium poly(2-acrylamido-2-methylpropane-sulfonate) (NaPAMS) (Figure 1). In the present work, we focus our study on the interaction in the dilute concentration region and above the isoelectric point of the protein where the net charge of gelatin is negative

* To whom correspondence should be addressed.

†Present address: Department of Chemistry, The University of North Carolina, Chapel Hill, NC 27599-3290.

© Abstract published in *Advance ACS Abstracts*, May 15, 1997.

($\text{pH} > \text{pH}_{\text{iso}}$). Normally one would expect an electrostatic repulsion between the polyanion and the net negatively charged gelatin. Despite such expectation, we will demonstrate that complexes can be formed between the two components. The ampholytic gelatin molecules are polarized in the electric field of a polyanion, and complexation between gelatin and the polyanion is driven by polarization-induced attraction.

To quantify complex formation in terms of molecular weight and stoichiometry of the complex, the second virial coefficient, the radius of gyration, and the hydrodynamic radius, we have conducted static- and dynamic-light-scattering experiments. In order to demonstrate that the complex is an identifiable and stable species, separation techniques such as differential size-exclusion chromatography (SEC) and flow field-flow fractionation were utilized, and the results will be reported elsewhere.²³ Under certain solution conditions, however, phase separation can be readily induced. In such cases, we have investigated this phenomena by turbidimetric titration, sedimentation, and fluorescence techniques.²⁴

The focus of this paper is on the light-scattering results and comparison of solution behavior between the two systems, NaPSS/gelatin and NaPAMS/gelatin. Chain characteristics of gelatin and the parent polyelectrolytes are presented first, followed by complexation study of the two polyanions with gelatin. A polarization-induced mechanism for complexation will be proposed for discussing the extent of complexation as a function of pH, ionic strength, and charge density of the polyanion. We believe that characterization of structure and stability of the complexes is essential for understanding complexation mechanism and ultimately properties of the mixtures in the semidilute or concentrated solutions.

II. Experimental Section

A. Polymer Materials. The gelatin sample used in this work was provided by Dr. T. H. Whitesides, Eastman Kodak Company. It is a Type IV gelatin ($\text{pH}_{\text{iso}} = 4.9$) containing all the α , β , and γ chains. The sample has been deionized with a mixed-bed ion exchange resin and freeze dried.²⁵ The weight-average molecular weight (M_w) determined by static-light-scattering is 2.19×10^5 and the polydispersity index is 2.3.

For the homopolymer NaPSS, two narrow-molecular-weight-distribution samples were employed. These were purchased from Scientific Polymer Products, Inc. with $M_w = 5.05 \times 10^5$ and 1.2×10^6 and the polydispersity indices = 1.24 and 1.17, respectively. These samples were further dialyzed for 24 h with an Amicon diafiltration unit equipped with a 10 000 MW cutoff spiral membrane ultrafiltration cartridge, in conjunction with a Barnstead Nanopure ultrapure water system. The weight-average molecular weights determined by our light scattering in aqueous salt solution were 5.05×10^5 and 1.09×10^6 , respectively, for the above two samples.

The homopolymer NaPAMS was prepared by free radical polymerization in water. To a 1 L three-necked flask equipped with a stirrer and condenser was added 172.4 g of 58% sodium 2-acrylamido-2-methylpropanesulfonate solution and 160.9 g of distilled water. The solution was bubbled with nitrogen for 1 h and then placed in a 60 °C bath. The catalyst $\text{K}_2\text{S}_2\text{O}_8$ (0.128 g) was added, and the solution was stirred under nitrogen for 16 h. The viscous mixture was cooled and diluted with 500 mL of water to give a stock solution containing ~12% solids. The inherent viscosity of the polymer was 2.50 dL/g (at $C_p = 0.5\%$) in 0.1 M Na_2SO_4 .

In the present study, a narrow-molecular-weight-distribution fraction of NaPAMS was used. This was obtained by fractionating the above whole polymer employing a stepwise fractionation method using aqueous NaCl/ethanol as the solvent/nonsolvent system. The weight-average molecular weight of this particular fraction was determined by light scattering in aqueous solution and found to be 1.1×10^6 . The

polydispersity index of this fraction (1.3) was determined by using a Hewlett-Packard HP 1090M size-exclusion chromatography system with SynChropak GPC 4000 and 1000 columns connected to a refractive-index detector HP 1047A.

B. Light-Scattering Measurements. Static- and dynamic-light-scattering experiments were performed at 40 °C with a Brookhaven Laser Light-Scattering 2030 System equipped with a BI 200SM goniometer, an Excel 3000 argon ion laser tuned at 514.5 nm as the incident light, and a BI 2030AT digital correlator with 136 channels. A Wyatt optiLab 903 interferometric refractometer was used in conjunction with the BI 2030AT for measurement of the refractive increment dn/dc at the same wavelength. The Zimm plot routine was employed for the static-light-scattering runs for dilute solutions of pure polyanions and the gelatin/polyanion mixtures in aqueous salt solutions. To measure the hydrodynamic size of the polyanions or the complexes, the autocorrelation functions were analyzed by the CONTIN program.

Sample preparations for the light-scattering experiments were made as follows. For light-scattering runs of the pure gelatin solutions, a concentrated gelatin stock solution (1%) was first prepared by dissolving 100 mg of the deionized gelatin solid in 10 g sodium acetate (NaAc) buffer solution at 50 °C for 2 h at an appropriate NaAc concentration (C_{NaAc}) and pH. This stock solution was further diluted to 0.2% and filtered several times with 0.45 μm and then 0.2 μm Sterile Acrodisc disposable filters. A 1 mL sample solution was introduced into the light-scattering cuvette and subsequent dilutions were made in the same cuvette with a salt solution, which was prefiltered several times with a 0.1 μm filter.

For light-scattering runs of the pure polyelectrolyte solutions, a polymer stock solution (0.5%) was prepared by dissolving 100 mg of the polymer solid in 20 g of sodium acetate buffer solution at a given C_{NaAc} and pH. This stock solution was filtered several times with a 1.2 μm Sterile Acrodisc disposable filter. Filters with smaller pore sizes were not appropriate for the present high-molecular-weight polyelectrolytes, as the concentration and the light-scattering intensity at 90° of the solution were found to be reduced upon filtration. This polymer stock solution was subsequently diluted to less than 0.1% with the solvent (0.1 μm filtered) in a dust-free cuvette before proceeding with light-scattering measurements.

Much more dilute solutions were required for light-scattering experiments of the gelatin/polyanion mixed solutions, since the scattering intensity is greatly enhanced upon complexation. Typically, 1 mL of the prefiltered gelatin solution (<0.01%, diluted from the above 1% gelatin stock solution) was first introduced into a dust-free cuvette and an appropriate volume in μL portion of the 1.2 μm prefiltered polyanion stock solutions (either 0.5% or 0.1% as prepared above) was added to yield a desired gelatin/polyanion weight ratio r at a given C_{NaAc} and pH. Subsequent dilutions were made in the same cuvette with the 0.1 μm prefiltered solvent at the same C_{NaAc} and pH. Filtration of the complexed solution after mixing was not appropriate because of the possibility of eliminating the larger gelatin/polyanion complexes. It is important that light-scattering measurements for a given mixture with a complete Zimm plot should be conducted within 2–3 h to avoid possible aggregation of the complexes or deterioration of the gelatin sample. A skewed Zimm plot was observed for samples on prolonged standing (>24 h), or at high ionic strengths, or at $\text{pH} < \text{pH}_{\text{iso}}$, indicative of aggregation and coacervation.

C. Intrinsic-Viscosity Measurements. The intrinsic viscosities for the pure polyanions NaPSS and NaPAMS, in 0.01 N NaAc at pH 5.65, were determined at 25 °C by using an automated Ubbelohde viscometer purchased from Schott Gerate. The extrapolated intrinsic viscosity value was obtained by linear plots of reduced viscosity, as well as of inherent viscosity, vs polymer concentration.

III. Results and Discussion

A. Chain Characteristics of Gelatin. The light-scattering data for pure gelatin in various C_{NaAc} and pH are listed in Table 1. The weight-average molecular weight of 2.19×10^5 was an average value obtained from all M_w values (± 5 –7%) measured. At $\text{pH} > \text{pH}_{\text{iso}}$ (=4.9),

Table 1. Radii of Gyration R_g and Second Virial Coefficients A_2 of Gelatin in Various C_{NaAc} and pH at 40 °C

C_{NaAc} (N)	pH	R_g (nm)	A_2 (10^{-4} cm ³ mol g ⁻²)
0.001	4.2	30	23
	6.0	35	28
	6.8	37	39
	7.2	33	52
	8.0	35	49
0.01	6.5	31	8.6
	7.4	32	19
	9.0	29	14
0.1	4.7	23	1.5
	6.5	20	1.6
	10.0	18	2.5

^a dn/dc value used for the gelatin solution is 0.18 mL/g. ^b The weight-average molecular weight of 2.19×10^5 was taken as the average of all values obtained in various C_{NaAc} .

there are more negative charges than positive charges on a gelatin molecule (see Figure 2.4 in ref 26). Therefore, the radius of gyration and the second virial coefficient are expected to decrease with increasing ionic strength, similar to the behavior of a linear polyelectrolyte. This trend is indicated by the data shown in Table 1. The variation in R_g with pH at a given salt concentration was difficult to detect, however, within the experimental accuracy of light scattering ($\pm 10\%$). On the other hand, the increase in A_2 with increasing pH at a given ionic strength is measurable in all three C_{NaAc} . The result is consistent with the behavior of an ionizable anionic polyelectrolyte for which its charge increases with pH, leading to a larger A_2 value.

By using a static-light-scattering technique, Pezron, Djabourov, and Leblond²⁷ also reported the following values for their lime-processed ossein-extracted gelatin in 0.1 N NaCl at pH 7.0 and 50 °C: $M_w = 1.9 \times 10^5$, $R_g = 35 \pm 4$ nm, and $A_2 = (3 \pm 1) \times 10^{-4}$ cm³ mol g⁻². Our R_g values in 0.1 N NaAc are smaller, but the A_2 values are comparable to their data (see Table 1). The differences in the sources of gelatin and the degree of deionization may be the cause for this discrepancy.

B. Chain Characteristics of Sulfonated Polyelectrolytes in Salt Solutions. Dilute solution behavior of polyelectrolytes in salt solutions were well characterized by light scattering and intrinsic viscosity and reported previously for the present two polymers NaPSS²⁸ and NaPAMS.²⁹ Comparison of hydrodynamic coil expansions of the two polyelectrolytes in aqueous salt solutions can be made based on the exponents of the following reported Mark-Houwink equations, e.g.,

$$[\eta] = 0.28 \times 10^{-4} M^{0.89} \text{ (NaPSS in } C_{\text{NaCl}} = 0.01 \text{ N)}^{28}$$

$$[\eta] = 2.04 \times 10^{-4} M^{0.50} \text{ (NaPSS in } C_{\text{NaCl}} = 4.17 \text{ N)}^{28}$$

$$[\eta] = 0.83 \times 10^{-5} M^{1.00} \text{ (NaPAMS in } C_{\text{NaCl}} = 0.01 \text{ N)}^{29}$$

$$[\eta] = 5.31 \times 10^{-5} M^{0.72} \text{ (NaPAMS in } C_{\text{NaCl}} = 5.00 \text{ N)}^{29}$$

The above equations were derived from intrinsic-viscosity data (dL/g) for several polymer fractions with weight-average molecular weights ranging from 10^5 to 2×10^6 . The values of the exponents in 0.01 N (0.89 for NaPSS and 1.00 for NaPAMS, respectively) indicate that, in this molecular-weight range studied, NaPSS is less extended than NaPAMS. While the θ condition is

Table 2. Radii of Gyration R_g and Second Virial Coefficients A_2 of NaPSS and NaPAMS in Various C_{NaAc} at pH = 7.0 and 40 °C

C_{NaAc} (N)	R_g (nm)	A_2 (10^{-4} cm ³ mol g ⁻²)
NaPSS (1.09×10^6)		
0.01	108	18
0.05	76	2.0
0.1	63	0.9
0.2	65	1.0
0.3	63	1.1
NaPAMS (1.1×10^6)		
0.01	90	21
0.05	82	11
0.1	77	11
0.2	66	11
0.5	61	9.4

^a dn/dc value for NaPSS is 0.18 mL/g, independent of C_{NaAc} . ^b dn/dc values for NaPAMS are 0.145 mL/g at 0.001–0.1 N and 0.14–0.135 mL/g at 0.1–0.5 N NaAc.

4.17 N for NaPSS with an exponent value of 0.50, the corresponding exponent value is 0.72 for NaPAMS, even in a slightly higher salt concentration of 5.00 N. A θ condition cannot be reached with the latter polyanion even in concentrated aqueous salt solution of $C_{\text{NaCl}} > 5.00$ N. This is attributed to the more hydrophilic acrylamide-containing monomer in NaPAMS vs the hydrophobic styrene-containing monomer in NaPSS. Our direct measurements of intrinsic viscosities for the present two narrow-molecular-weight fractions (dp = degree of polymerization),

$$[\eta] = 6.5 \text{ dL/g [NaPSS, } M_w = 1.09 \times 10^6 \text{ (dp = 5400) in } C_{\text{NaAc}} = 0.01 \text{ N]}$$

$$[\eta] = 7.1 \text{ dL/g [NaPAMS, } M_w = 1.10 \times 10^6 \text{ (dp = 4800) in } C_{\text{NaAc}} = 0.01 \text{ N]}$$

also confirmed that, for a given chain length or dp, the NaPSS chain is less extended with smaller hydrodynamic volume than that of NaPAMS.

The static-light-scattering data at 40 °C for the same pair of NaPSS and NaPAMS polyanions as a function of C_{NaAc} are summarized in Table 2. Within the experimental accuracy of light scattering for determining R_g ($\pm 10\%$), the static dimensions of the two chains in a given C_{NaAc} or as a function of C_{NaAc} are not greatly different from each other. On the contrary, the second virial coefficients are much higher for NaPAMS than those for NaPSS in the same C_{NaAc} range. This is consistent with the higher Mark-Houwink exponent for NaPAMS than that for NaPSS discussed above, suggesting that the aqueous salt solution is a better solvent for the NaPAMS polyanion.

Differences in coil sizes and the excluded volume effects of the two polymers have direct impact on their interactions with gelatin. This will be discussed later after section C.

C. Formation of Soluble Gelatin/Polyanion Complexes. Despite the expected electrostatic repulsion between the negatively charged polyanion and the net negatively charged gelatin at pH $>$ pH_{iso}, the enhanced scattering intensity upon mixing provides evidence for complex formation. This enhanced scattering can be detected at very low concentrations. Plotted in Figure 2 is the relative scattering intensity at 90° vs feed weight ratio of gelatin to polyanion r for mixed solutions of gelatin and NaPSS in 0.01 N NaAc at pH = 5.65 and 40 °C, where the concentration of gelatin was kept constant at 0.05%. The intensities of the two individual

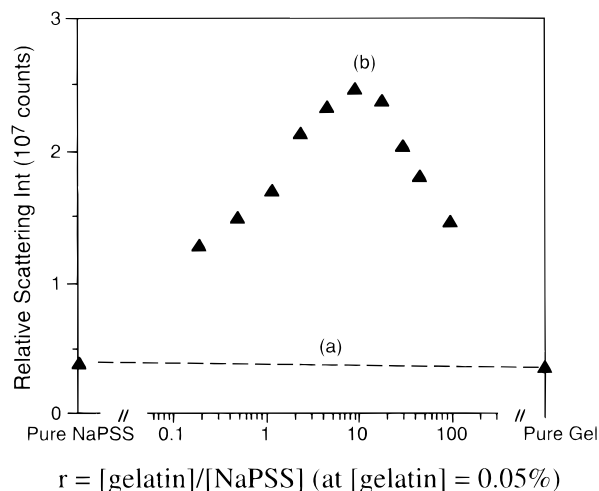


Figure 2. Relative light-scattering intensity vs r for gelatin/NaPSS in 0.01 N NaAc at pH 5.65, 40 °C.

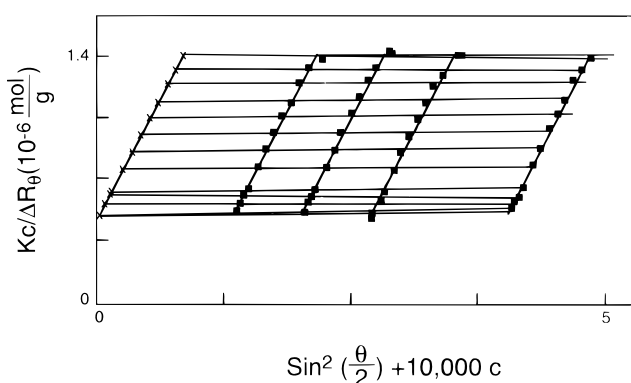


Figure 3. Zimm plot for a mixture of gelatin/NaPSS ($r = 50$) in 0.05 N NaAc at pH 7.8, 40 °C.

components are very low. A dotted straight line (line (a)) in Figure 2 represents the total intensities for the mixtures if there were no interaction between the two components. In contrast, our measurements show that intensity is greatly enhanced upon mixing. The initial increase in intensity from the pure gelatin side (right-hand side of the x -axis) to $r = 12$ is a result of complexation upon addition of polyanion. The total intensity is derived from the gelatin-saturated complexed chain plus the excess free gelatin. Further increase in polyanion concentration (i.e., decrease in r) below $r = 12$ results in depletion of the bound gelatin on the polyanion chain (forming unsaturated complexes) and hence decrease in intensity.

In order to quantify the molecular weights of the complexes at various r values, the conventional static-light-scattering technique is much more informative than the intensity data presented in Figure 2. As an example, a normal Zimm plot was obtained and shown in Figure 3. This normal behavior in the Zimm plot suggests the absence of aggregation within 2–3 h upon mixing the components. A skewed Zimm plot was obtained, however, for some samples on prolonged standing (>24 h), at higher ionic strengths, or at pH < pH_{iso}, where aggregation between complexes or coacervation becomes pronounced. Several approaches have been adopted by other workers,^{11,15,19} for light-scattering characterization of polyelectrolyte complexes. Kabanov et al.¹¹ studied complex formation for a nonstoichiometric mixture of a long-chain polyanion and a much shorter oppositely charged chain. They assumed that the complex is the only species present and utilized the conventional Zimm plot procedure to obtain the weight-

average molecular weight, radius of gyration, and the second virial coefficient of the complex. Different analyses of the light-scattering data were also employed by Dautzenberg et al.,¹⁵ Dubin et al.¹⁹ for studying protein/polyelectrolyte and surfactant/polyelectrolyte complexation.³⁰

In the present work, we have taken the following approach in treating our light-scattering data. The stoichiometry and molecular weight of the complex for a mixture of gelatin and polyanion at a given r can be calculated according to the following scheme, using the measured “apparent” weight-average molecular weight derived from the conventional Zimm plot procedure. Since the number of charges on gelatin is much smaller than that on the polyelectrolyte chains used in this study, we can consider a complex as composed of x gelatin molecules adsorbed onto a single polyelectrolyte chain. Below we assume that only two species are present in the mixture: the complex and the free gelatin.

Let the molecular weight of gelatin and polyelectrolyte chains be M_g and M_p and the corresponding initial concentrations be c_g and c_p , respectively. We define the feed weight ratio of gelatin to polyanion as

$$r = \frac{c_g}{c_p}$$

the molecular weight of the complex as

$$M_c = M_p + xM_g$$

and the stoichiometry of the complex as

$$r_c = x \frac{M_g}{M_p}$$

If all polyelectrolyte chains are utilized in complexing, the concentration of bound gelatin is $r_c c_p$ and the concentration of free gelatin is

$$c_{fg} = c_g - r_c c_p$$

The concentration of the complex is then

$$c_c = c_p + r_c c_p$$

By substitutions using the above relationships, we obtain the following expression for the weight-average molecular weight of the mixture of complexes and free gelatin molecules as

$$M_w = \frac{M_g c_{fg} + M_c c_c}{c_c + c_{fg}} = \frac{(r - r_c)M_g + (1 + r_c)^2 M_p}{1 + r} \quad (1)$$

The value for M_w can be measured directly as the “apparent” weight-average molecular weight, M_w (app), derived from the Zimm plot at a given r , while M_g and M_p can be measured independently for the pure gelatin and the polymer. Hence the complex stoichiometry r_c can be calculated as follows:

$$r_c = \frac{M_g}{2M_p} - 1 + \left[\frac{M_g^2}{4M_p^2} + \frac{(M_w - M_g)(1 + r)}{M_p} \right]^{1/2} \quad (2)$$

Consequently the values for x and the molecular weight of the complex M_c can be calculated. Since the larger molecules contribute most of the scattering even at $r = 200$, the measured radius of gyration and the

Table 3. Light-Scattering Data, Calculated Complex Stoichiometry r_c , and Number of Gelatin Molecules per Chain x for Gelatin/NaPSS in 0.01 N NaAc at pH = 5.65 and 40 °C

r (w/w)	$M_w(\text{app})$ (10^5)	R_g (nm)	A_2 (10^{-4} cm ³ mol g ⁻²)	r_c (w/w)	x (no. of gelatin molecules per chain)
NaPSS (1.09×10^6)					
200	22.3	103	-0.77	18.36	91.37
100	41.3	116	-0.69	18.14	90.27
99	34.6	123	-0.50	16.34	81.35
50	50.4	120	-0.09	14.05	70.57
32.3	54.2	132	-0.41	11.71	58.26
30	50.6	129	0.06	10.84	53.93
19	56.1	121	-0.07	9.05	45.03
13.33	62.8	124	0.27	8.03	39.95
12.33	60.5	123	-0.80	7.55	37.56
12	68.0	113	0.16	7.96	39.62
10.42	62.1	120	-0.13	7.02	34.96
9	62.5	123	-0.03	6.54	32.55
7	59.7	122	-0.82	5.60	27.86
6	60.5	107	-0.63	5.22	25.98
5.67	62.6	118	0.39	5.18	25.79
4	47.0	104	0.62	3.64	18.09
2.5	44.5	118	0.77	2.79	13.88
1.86	45.8	123	4.6	2.49	12.37
1	32.9	120	3.0	1.48	7.35
0.25	12.8	90	5.5	0.208	1.04
pure NaPSS					
10.9	108	18			
NaPSS (5.05×10^5)					
196	11.6	77	-0.65	18.38	42.38
98	18.0	70	-0.49	16.82	38.79
50	27.4	75	-0.48	15.17	34.99
20	31.8	68	-0.25	10.32	23.79
12.3	33.0	81	-0.21	8.23	18.97
12.3	32.0	77	-0.26	8.08	18.63
12.0	30.9	67	-0.25	7.82	18.02
6	25.8	64	0.80	4.94	11.40
4	20.9	61	1.15	3.53	8.13
3	16.9	63	0.40	2.64	6.08
1	10.7	57	2.4	1.07	2.46
1	9.73	58	2.4	0.96	2.20
pure NaPSS					
5.05	50	12			

^a dn/dc value for Gelatin/NaPSS is 0.18 mL/g, independent of r and C_{NaAc} .

second virial coefficient are similar to those for the complex species.

1. Gelatin/NaPSS Complex. Light-scattering data for the gelatin/NaPSS mixtures in 0.01 N NaAc at pH 5.65 and 40 °C are summarized in Table 3. The "apparent" weight-average molecular weights of the mixtures $M_w(\text{app})$, are plotted in Figure 4 vs r , where $M_w(\text{app})$'s are derived directly from the Zimm plot. Data points for the two gelatin/NaPSS (1.09×10^6 and 5.05×10^5) systems are shown as curves a and b, respectively. The general shape of the curves are similar to the intensity curve shown as curve b in Figure 2. The corresponding calculated complex stoichiometry r_c vs r are presented in Figure 5. The overlap of the data points for the two molecular weights of NaPSS shown in Figure 5 clearly indicates that the stoichiometry of the complex is independent of the NaPSS chain length. A straight line ($r_c = r$) is drawn in Figure 5, and deviation of the data points from this line indicates the nonstoichiometric complexation in the mixture. Evidently, in the low r region for $r \leq 5 \sim 6$, $r_c = r$. This suggests that virtually all gelatin molecules added are bound to the polyanion chain. This finding will be verified later by an independent technique, the differential size-exclusion chromatography.²³ The amount of bound gelatin continues to increase with increasing

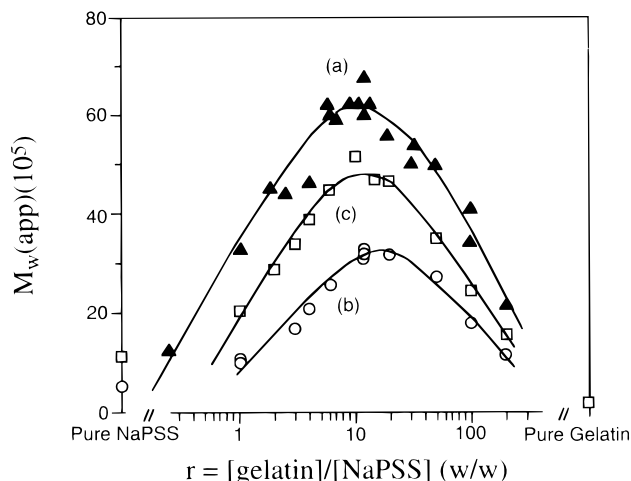


Figure 4. Apparent weight-average molecular weight $M_w(\text{app})$ vs r for (a) gelatin/NaPSS (1.09×10^6) (\blacktriangle), (b) gelatin/NaPSS (5.05×10^5) (\circ), and (c) gelatin/NaPAMS (1.1×10^6) (\square) in 0.01 N NaAc at pH 5.65, 40 °C.

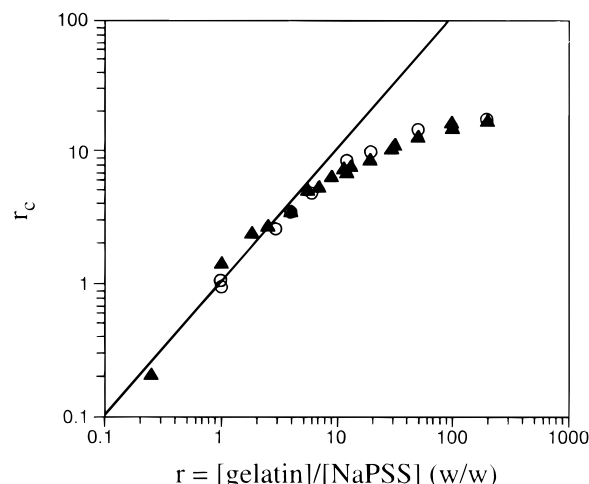


Figure 5. Complex stoichiometry r_c vs r for gelatin/NaPSS (1.09×10^6) (\blacktriangle) (5.05×10^5) (\circ) in 0.01 N NaAc at pH 5.65, 40 °C.

r above 5 \sim 6, but a saturation level is reached around $r_c = 18.5$ at $r = 200$. Experimental data beyond $r = 200$ are less reliable because of the decreasing intensity and increasing free gelatin present in the mixed solution.

The negative values of the second virial coefficient A_2 for $r > 6$ (see Table 3) show that attraction between complexed chains increases with gelatin saturation, an indication of the instability of the complex in solution. In fact, increased scattering intensity was observed for the dilute mixtures upon prolonged standing (> 24 h), resulting from complex–complex aggregation. This means that the tendency for complex–complex aggregation is enhanced when more gelatin molecules are bound to the polyanion. We have observed that precipitation occurs more readily at higher concentration of the mixture, depending on the concentration of the mixture, the feed composition r , ionic strength, and pH. This phenomenon was investigated in our phase behavior study.²⁴

An alternative representation of complex formation is shown as the plot of M_c vs r in Figure 6 for gelatin/NaPSS (1.09×10^6) (curve (a)). Considering the large molecular-weight buildup of the complex upon gelatin binding (i.e., 20-fold), and the slight increase in R_g (15%) (see Table 3), the structure of the complex must be denser than that of the parent chain.

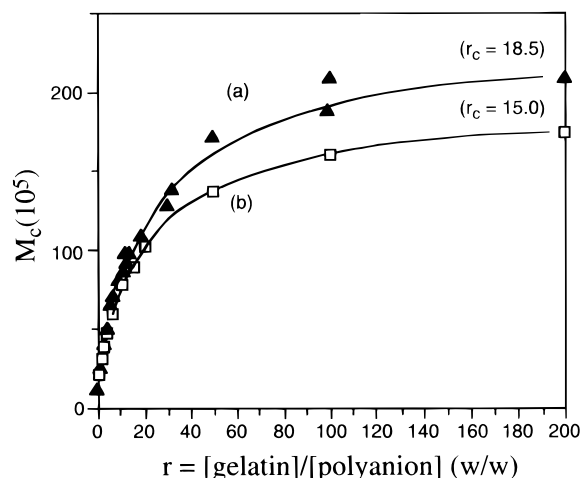


Figure 6. Complex molecular weight M_c vs r for (a) gelatin/NaPSS (1.09×10^6) (\blacktriangle) and (b) gelatin/NaPAMS (1.1×10^6) (\square) in 0.01 N NaAc at pH 5.65, 40 °C (the curves were drawn through the data points for visual aids).

Table 4. Light-Scattering Data, Calculated Complex Stoichiometry r_c , and Number of Gelatin Molecules per Chain x for Gelatin/NaPAMS in 0.01 N NaAc at pH = 5.65 and 40 °C

r (w/w)	$M_w(\text{app})$ (10^5)	R_g (nm)	A_2 (10^{-4} cm ³ mol g ⁻²)	r_c (w/w)	x (no. of gelatin molecules per chain)
NaPAMS (1.1×10^6)					
200	15.8	90	-0.78	14.87	74.69
100	24.8	98	-0.34	13.51	67.85
50	35.3	101	-0.34	11.49	57.71
20	47.0	97	0.05	8.35	41.94
15	47.2	103	0.18	7.19	36.12
10	51.8	101	0.24	6.14	30.86
6	45.0	102	0.22	4.32	21.70
4	39.1	97	0.53	3.20	16.06
3	33.9	92	0.008	2.50	12.54
2	28.7	89	0.95	1.79	8.99
1	20.4	93	3.4	0.92	4.63
pure NaPAMS					
	11.0	90	21		

^a dn/dc value for Gelatin/NaPAMS ranges from 0.178 mL/g, at $r = 200$, to 0.16 mL/g, at $r = 1$.

2. Gelatin/NaPAMS Complex. Light-scattering data for the gelatin/NaPAMS (1.1×10^6) mixtures in 0.01 N NaAc at pH 5.65 and 40 °C are listed in Table 4. To compare with those of gelatin/NaPSS, plots of $M_w(\text{app})$ vs r , as well as M_c vs r , are included in Figures 4 (curve (c)) and Figure 6 (curve (b)), respectively. Although the molecular weights of the two parent polyanions are identical, the values of $M_w(\text{app})$ or M_c for gelatin/NaPAMS mixtures are consistently lower than those for gelatin/NaPSS. The saturation level (see Figure 6) is approximately around $r_c = 15.0$ at $r = 200$ for gelatin/NaPAMS (i.e., 64 monomers/gelatin), slightly smaller than the value of $r_c = 18.5$ for gelatin/NaPSS (i.e., 57 styrene sulfonate monomers/gelatin).

Similar to the gelatin/NaPSS system, negative second virial coefficient was also obtained upon complexation for gelatin/NaPAMS, but at a higher complex stoichiometry (see Table 4). This indicates that attraction between the complexed chains is less pronounced, or the aqueous medium is a better solvent for the gelatin/NaPAMS system. This finding is consistent with the single-phase behavior observed for the latter system.²⁴ On the basis of the small increase in R_g (+10%) (Table 4) and the large complex molecular weights (Figure 6), the structure of the gelatin/NaPAMS complex is also denser than that of the parent NaPAMS chain.

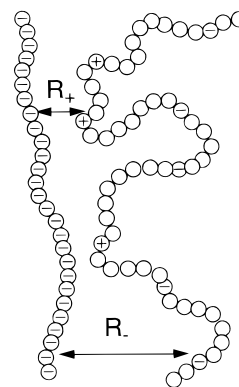


Figure 7. Overall configuration of the complex between a segment of the polyanion and a gelatin molecule.

Table 5. Chain Characteristics of the Gelatin/Polyanion Complexes in 0.01 N NaAc at pH = 5.65 and 40 °C

complexes	gelatin/NaPSS (1.09×10^6)	gelatin/NaPAMS (1.1×10^6)
stoichiometry (r_c)	18.5 (at $r = 200$) (or 1 gelatin/ 57 monomers)	15 (at $r = 200$) (or 1 gelatin/ 64 monomers)
M_c	22×10^6	17×10^6
R_g complex	120 nm	100 nm
R_g polyanion	108 nm	90 nm
R_h complex	70 nm	60 nm
R_h/R_g complex	0.58	0.60
A_2	more negative	less negative
$M_c/N(4\pi/3)R_g^3$	0.005 g/cm ³	0.006 g/cm ³

D. Comparison of Solution Behavior for Gelatin/NaPSS vs Gelatin/NaPAMS. 1. Complex Formation in 0.01 N NaAc at pH 5.65 and 40 °C. Results for chain characteristics of the two complexes in 0.01 N NaAc at pH 5.65 and 40 °C are summarized in Table 5. The extent of gelatin binding to the polyanion for gelatin/NaPSS ($r_c = 18.5$ or 1 gelatin/57 monomer) is slightly larger than that for gelatin/NaPAMS ($r_c = 15.0$ or 1 gelatin/64 monomer).

The total numbers of ionic groups per gelatin with a molecular weight of 2×10^5 are estimated to be 188 mole of base/gelatin and 260 mole of acid/gelatin.³¹ At pH = 5.65, the net negative charge per gelatin is estimated to be -40 for a gelatin with a molecular weight of 2×10^5 , according to Figure 2.4 in ref 26. Assuming all cationic sites are ionized at pH = 5.65, there will be approximately 188 positive charges (Q_+) and 228 negative charges (Q_-) for each gelatin associated with a segment of 57 sulfonate monomers for NaPSS or 64 monomers for NaPAMS, respectively. Even though the net charge on gelatin is negative (-40), attraction between the negatively charged polyanion and gelatin can occur through favorable chain configuration of gelatin as depicted in Figure 7. The electric field of the polyanion polarizes gelatin, bringing positively charged units closer to the polyanion (at average distance R_+) and moving negatively charged units further away from it (at average distance $R_- > R_+$). As long as the ratio of these distances is greater than the corresponding charge ratio, i.e.,

$$\frac{R_-}{R_+} > \frac{Q_-}{Q_+} \approx 1.2 \quad (3)$$

the overall coulombic interaction between gelatin and polyanion is attractive (i.e., $Q_+/R_+ > Q_-/R_-$). In fact, it is the presence of the net negative charge on the complex that provides the stability of the complex.

The extent of gelatin binding may be related to the overall chain configuration and the monomer chemical

structure of the parent polyelectrolyte. As discussed earlier in the intrinsic-viscosity results in section B, NaPSS is less extended compared to NaPAMS. This can be explained by the greater hydrophobicity of NaPSS, leading to more compact conformations than the conformation of NaPAMS. Thus the more compact NaPSS coil has higher charge density (i.e., larger number of charges per unit length),³² and therefore greater field strength, polarizing gelatin and creating attraction. This greater charge density in NaPSS is attributed to the hydrophobic nature of the styrene-containing monomer. Consequently, the number of gelatin molecules that bind to a given polymer chain is larger for NaPSS than that for NaPAMS. Another polyelectrolyte of interest for such comparison would be sodium poly(vinylsulfonate) (NaPVS).³³ Unfortunately, complete intrinsic viscosity-molecular weight relationship is not available because of synthetic difficulty in preparing high-molecular-weight NaPVS. Among the three polyanions, we expect that charge density and hence the extent of gelatin binding should follow the decreasing order NaPVS > NaPSS > NaPAMS.

As we have discussed earlier in section C, the structures of the gelatin/NaPSS and gelatin/NaPAMS complexes are denser than those of the corresponding parent polymers. This can be seen by their larger molecular weights and yet comparable sizes to those of their parent polymers. Also listed in Table 5 are the hydrodynamic radii of the complexes as determined by dynamic light scattering. The values for the ratio R_h/R_g are 0.58 for gelatin/NaPSS and 0.60 for gelatin/NaPAMS, respectively. This implies that the complexes behave similarly to a partial-draining coil rather than a collapsed non-draining sphere.^{34,35} This finding is consistent with the relatively low local concentrations inside the complex coil estimated as follows. The mass per unit coil volume for the complex can be calculated from the measured values of M_c and R_g , and is listed for each complex in Table 5 (i.e., 0.005 and 0.006 g/cm³ for the gelatin/NaPSS and gelatin/NaPAMS complexes, respectively). These small values reveal that more than 99% of the volume inside the complex is occupied by water molecules. Thus a partial-draining coil is a realistic model for the present gelatin/polyelectrolyte complexes.

In the very dilute solution region, the short-term stability of the complex is a result of repulsion between the negatively charged complexed chains. This is the very reason that static-light-scattering experiments can be performed on these systems. The unsaturated complexes ($r_c < 5.22$ for gelatin/NaPSS and $r_c < 11.49$ for gelatin/NaPAMS) are relatively stable, consistent with the observed positive values of A_2 shown in Tables 3 and 4. The saturated complexes, on the other hand, show negative A_2 values, indicating attraction between the complexed chains. These results can be interpreted by the following model proposed for the complex configuration. In the low-stoichiometric-complex region where the polyanion is not saturated with gelatin molecules, the gelatin chain is likely to be bound with its backbone lying "flat" along the polyanion chain axis with fewer free segments or loops extending into the aqueous phase. Aggregation between two complexed chains caused by the "bridging" of one gelatin is less probable in dilute solution when the two complexes are far apart. In the high-stoichiometric-complex region, the larger number of bound gelatin chains have to rearrange themselves in order to accommodate for the limited space along the polyanion backbone. It is expected that there are more free gelatin loops extend-

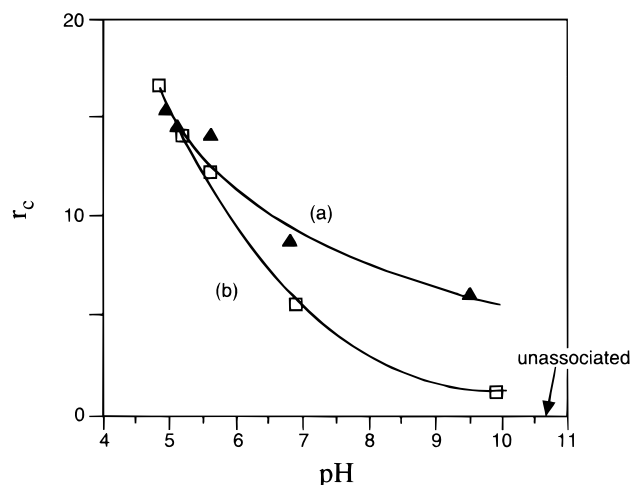


Figure 8. Complex stoichiometry r_c vs pH for (a) gelatin/NaPSS (1.09×10^6) (\blacktriangle) and (b) gelatin/NaPAMS (1.1×10^6) (\square) at $r = 50$ in 0.01 N NaAc, 40 °C (the curves were drawn through the data points for visual aids).

ing into the aqueous phase for a given complex. Hence the attraction between two complexed chains can occur more readily by "bridging" of one bound gelatin, resulting in negative values of A_2 .

In the semidilute or concentrated solution region above the overlap concentrations of gelatin (>0.5%) and the polyanion, the conformation of the bound gelatin may not play as an important role in complex aggregation. Complex-complex aggregation leading to phase separation was observed for the low-stoichiometric-complex region (i.e. $r < 10$), where many of the polyanion sites are not occupied by gelatin. The "bridging" between two unsaturated complexed chains by one gelatin is expected as the two chains are brought closer by concentration increase. For the high-saturation region, all binding sites of the polyanion are occupied by gelatin, and "bridging" is less probable. Hence a stable single phase is observed.²⁴

2. Effect of pH on Complex Formation. The stabilities of the complexes as a function of pH are presented in Figure 8 as complex stoichiometry r_c vs pH for gelatin/NaPSS (1.09×10^6) (curve (a)) and gelatin/NaPAMS (1.1×10^6) (curve (b)) at $r = 50$ in 0.01 N NaAc at 40 °C. For gelatin/NaPSS mixtures, complexation decreases with increasing pH, but remains measurable even at pH = 9.5 with $r_c = 6.15$. Light-scattering experiments with samples having pH below pH_{iso} were difficult to perform because of rapid interchain aggregation, eventually leading to phase separation. For gelatin/NaPAMS mixtures, complexation also decreases with increasing pH, but the two components were no longer associated at pH > 10 (i.e., $r_c \rightarrow 0$). On the other hand, aggregation was not observed even at pH = 4.84 ($< pH_{iso}$) and the stoichiometry of the complex r_c was found to be 16.5. The general conclusion is that complexation is reduced with increasing pH, a result of increasing repulsion between the negatively charged polyanions and the increasingly more negatively charged gelatin. Complexation is weaker for gelatin/NaPAMS than for gelatin/NaPSS. Complete dissociation was observed for gelatin/NaPAMS at high pH (>10).

3. Effect of Salt Concentration on Complex Formation. Enhanced turbidity, eventually leading to aggregation upon prolonged standing (>24 h), was observed at $C_{NaAc} > 0.01$ N for gelatin/NaPSS at $r \leq 10$, resulting from interchain attraction. Hence, studies of the effect of salt concentration on complexation were possible only at a high feed ratio (e.g., $r = 50$). Plots of

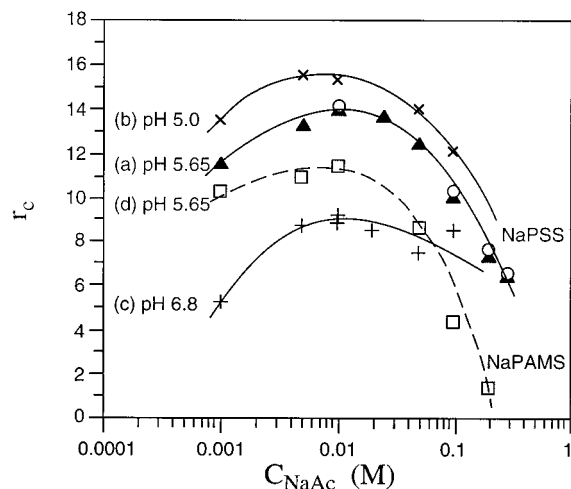


Figure 9. Complex stoichiometry r_c vs C_{NaAc} at $r = 50$, 40°C for gelatin/NaPSS at (a) pH 5.65 ($M_w = 1.09 \times 10^6$) (\blacktriangle) ($M_w = 5.05 \times 10^5$) (\circ), (b) pH 5.0 ($M_w = 1.09 \times 10^6$) (\times), (c) pH 6.8 ($M_w = 1.09 \times 10^6$) ($+$), and for gelatin/NaPAMS ($M_w = 1.1 \times 10^6$) at (d) pH 5.65 (\square) (the solid curves for gelatin/NaPSS (curves a, b, and c) and broken curve for gelatin/NaPAMS (d) were drawn through the data points for visual aids).

r_c vs C_{NaAc} for the two gelatin/NaPSS systems (1.09×10^6 and 5.05×10^5) systems at pH = 5.65 and 40°C are shown as curve (a) in Figure 9. The overlap of the data points for curve (a) demonstrates that changes in complex stoichiometry with C_{NaAc} are independent of molecular weight of the polyanion.

The effect of C_{NaAc} on complexation was also studied as a function of pH (5.0, 5.65, and 6.8) for gelatin/NaPSS (1.09×10^6) at $r = 50$ and shown as curves (b), (a), and (c), respectively, in Figure 9.

The general trend for r_c vs C_{NaAc} can be rationalized in terms of screening effect of electrolyte. The presence of salt leads to screening of Coulombic interaction by the factor³⁶ $\exp(-R/R_D)$, where R is the distance between the charges and R_D is the Debye screening length ($R_D = (8\pi l_B C_s)^{-1/2}$), with l_B being the Bjerrum length ($\sim 7 \text{ \AA}$ in water) and C_s the concentration of the monovalent salt. For example, at $C_s = 0.01 \text{ N}$, R_D is calculated to be 30 \AA according to the above relation. Because of the evidence for complexation, we have previously assumed that the average distance between the positive charges on gelatin and the polyanion R_+ (see Figure 7) is shorter than that between the negative charges on gelatin and the polyanion, R_- . This interaction can be described³⁶ by

$$U = -Q_p \left(\frac{Q_+}{R_+} e^{-R_+/R_D} - \frac{Q_-}{R_-} e^{-R_-/R_D} \right) \quad (4)$$

where Q_p is the charge of the segment of the polyanion associated with a gelatin molecule which contains Q_+ positive charges and Q_- negative charges. Thus the interactions in the three concentration regions as shown by the data in Figure 9 can be rationalized as follows: (i) At very low salt concentration ($C_{\text{NaAc}} < 0.005 \text{ N}$), $R_D > R_- > R_+$, and neither attraction nor repulsion are screened. The overall interaction is attractive, even though the net charge on gelatin is negative. This is caused by the induced polarization of the charges on gelatin, leading to a smaller distance R_+ between the positive charges on gelatin and polyanion as depicted in Figure 7.

(ii) At intermediate salt concentration ($0.005 < C_{\text{NaAc}} < 0.01 \text{ N}$), $R_+ < R_D < R_-$, and repulsion between polyanion and the negative charges on gelatin is par-

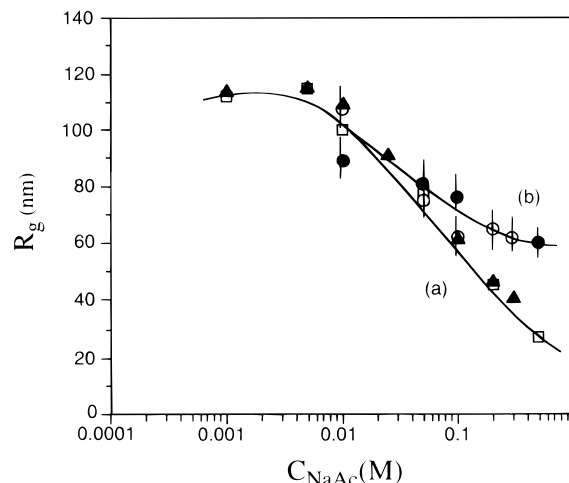


Figure 10. Radius of gyration R_g vs C_{NaAc} at pH 5.65, 40°C for (a) complexes of gelatin/NaPSS (1.09×10^6) (\blacktriangle) and gelatin/NaPAMS (1.1×10^6) (\square) at $r = 50$ and (b) pure polyanions NaPSS (1.09×10^6) (\circ) and NaPAMS (1.1×10^6) (\bullet) including experimental error bars (the curves were drawn through the data points for visual aids).

tially screened, while the attraction between the positive charges on gelatin and polyanion is almost unscreened. In this region, the overall attraction between gelatin and polyanion is the strongest as can be seen from the maxima in the complex stoichiometry shown in Figure 9.

(iii) At higher salt concentration ($C_{\text{NaAc}} > 0.01 \text{ N}$), the Debye length $R_D < R_+ < R_-$, and both repulsion and attraction are screened. Since complexation is caused by Coulombic attraction, it is significantly reduced with increasing salt concentration C_{NaAc} .

Note that the position of the maxima of complex stoichiometry corresponding to $0.005 < C_{\text{NaAc}} < 0.01 \text{ N}$ gives us a length scale for the average distance between charges on gelatin and polyanion. We estimated³⁷ $R_+ \sim 20\text{--}30 \text{ \AA}$ and $R_- \sim 40\text{--}50 \text{ \AA}$, which is consistent with the attractive condition described by eq 3. These length scales are comparable to the average distance between two neighboring charges on gelatin ($\sim 50 \text{ \AA}$). The latter was estimated from the measured radius of gyration and the total number of positive and negative charges of a gelatin molecule, assuming a freely jointed Gaussian coil. A possible configuration of a gelatin molecule in a complex may consist of loops of size $\sim 50 \text{ \AA}$ along the polyanion chain with negative charges distributed on the outside and positive charges on the inside part of the loops as depicted in Figure 7. The interplay between the repulsion and attraction appears to be an important and characteristic phenomenon associated with interactions of amphoteric polymers.

Shown in Figure 10 are the plots for R_g vs C_{NaAc} for the gelatin/NaPSS (1.09×10^6) and gelatin/NaPAMS (1.1×10^6) complexes (curve (a)) and the NaPSS (1.09×10^6) and NaPAMS (1.1×10^6) parent polyanions (curve (b)), respectively, at pH = 5.65 and 40°C . For $0.01 < C_{\text{NaAc}} < 0.1 \text{ N}$, the sizes for the complexes and the parent polyanions are comparable, but decrease with increasing C_{NaAc} . This is consistent with the behavior of a charged polymer. For $C_{\text{NaAc}} < 0.01 \text{ N}$, the size of the complex is not sensitive to C_{NaAc} , although the stoichiometry was shown to decrease slightly with decreasing C_{NaAc} (see Figure 9). Chain expansion for the parent polyanions below $C_{\text{NaAc}} = 0.01 \text{ N}$ is expected, however. Unfortunately, this is the region where experimental procedures with normal Zimm plot or the intrinsic viscosity plot cannot be readily applied. For

$C_{\text{NaAc}} > 0.1$ N, the complex size decreases below those values for the parent polyanions. Polymer intrachain coiling resulting from fewer bound gelatin at $C_{\text{NaAc}} > 0.1$ N (see Figure 9 for the smaller complex stoichiometry at $C_{\text{NaAc}} > 0.1$ N) may be the cause for the collapse of the complex.

Comparison of the extent of gelatin binding for the two polyanions as a function of C_{NaAc} is shown in Figure 9: gelatin/NaPSS (1.09×10^6) (curve (a)), gelatin/NaPAMS (1.1×10^6) (curve (d)). At $C_{\text{NaAc}} > 0.2$ N, the mixture of gelatin/NaPAMS remains clear but unassociated, in contrast to the partially complexed state for the gelatin/NaPSS system. For $0.2 > C_{\text{NaAc}} > 0.01$ N, the complex stoichiometry r_c reduces with increasing C_{NaAc} for both systems. These results also indicate that binding strength for gelatin/NaPAMS is weaker than that for gelatin/NaPSS. The maxima in r_c vs C_{NaAc} also occur at $C_{\text{NaAc}} = 0.01$ N for both complexes, corresponding to the Debye screening length of $R_D = 30$ Å.

IV. Conclusions

We have established experimental evidence for complexation between polyanions and a net negatively charged ampholytic gelatin. Our results suggest that electrostatic attraction is the main driving force for association. The gelatin molecules are polarized in the electric field of a polyelectrolyte chain. This polarization-induced attraction is believed to be the main mechanism for complexation. The weight-average molecular weights of the complexes upon saturation with gelatin molecules were found to increase 20- and 15-fold, respectively, for the two polyanions, NaPSS and NaPAMS. Nevertheless, the sizes of the complexes increase only slightly (+10%). The local concentration of chain segments inside the complexes was found to be much higher than those of the parent polyanions. On the other hand, more than 99% of the coil volume inside the complexes is occupied by water molecules. This finding is further substantiated by the measured R_h/R_g values (0.58–0.60), suggesting that the complexes behave similarly to a partial-draining random coil rather than a collapsed nondraining sphere.

Charge density is an important feature for the polyelectrolyte in determining its extent of gelatin binding. This feature can be manipulated by varying the chemical structures of the monomers (i.e., hydrophobicity, hydration, and the distance between the charge and the vinyl backbone) and the resulting polymer chain configuration. NaPSS is less extended than NaPAMS in aqueous salt solution, presumably resulting from the greater hydrophobicity of the styrene moiety in the former and the larger solvent affinity of the amide linkage in the latter. Therefore, NaPSS has a greater charge density and hence slightly larger extent of gelatin binding than NaPAMS.

Acknowledgment. We are grateful to Drs. T. H. Whitesides and R. H. Colby for helpful discussions.

References and Notes

- (1) (a) Tsuchida, E.; Abe, K. *Interactions between Macromolecules in Solution and Intermolecular Complexes*, Advances in Polymer Science 45; Springer-Verlag: New York, 1982. (b) Tsuchida, E. *J. Macromol. Sci., Pure Appl. Chem.* **1994**, A31 (1), 1.
- (2) *Polymer Preprints (ACS, Div. Polym. Chem.)* **1991**, 32 (1), 585–608.
- (3) Petrak, K. In *Polyelectrolytes, Science and Technology*; Hara, M., Ed.; Marcel Dekker: New York, 1993; p 265.
- (4) Mikulik, J.; Vinklerek, Z.; Vondruska, M. *Collect. Czech. Chem. Commun.* **1993**, 58 (4), 713.
- (5) Deasy, P. B. *Microencapsulation and Related Drug Process*; Marcel Dekker: Basel, 1984.
- (6) Guio, P.; Couvreur, P. *Polymeric Nanoparticles and Microspheres*; CRC Press: Boca Raton, Florida, 1986.
- (7) Albertsson, P. A. *Partition of Cell Particles and Macromolecules*, 2nd ed.; Wiley Intersciences: New York, 1971.
- (8) Kabanov, V. A.; Kabanov, A. V.; Astafyeva, I. N. *Polymer Preprints (ACS, Div. Polym. Chem.)* **1991**, 32 (1), 592.
- (9) Felgner, P. L. *Adv. Drug Delivery Rev.* **1990**, 5, 163.
- (10) *Flavor Encapsulation*; Risch, S. J., Reineccius, G. A., Eds.; ACS Symposium Series 370; American Chemical Society: Washington, DC, 1988.
- (11) Kabanov, V. A.; Zevin, A. B.; Mustafaev, M. I.; Kasaikin, V. A. In *Polymeric Amines and Ammonium Salts*; Goethals, E. J., Ed.; Pergamon Press: New York, 1980; p 173.
- (12) Hara, M.; Nakajima, A. *J. Polym. Sci., Part B: Polym. Phys.* **1989**, 27, 1043.
- (13) Domard, A.; Rinaudo, M. *Macromolecules* **1980**, 13, 896.
- (14) Frugier, D.; Audebert, R. *Polymer Preprints (ACS Div. Polym. Chem.)* **1991**, 32 (1), 590.
- (15) Dautzenberg, H.; Koetz, J.; Linow, K. J.; Philipp, B.; Rother, G. *Macromol. Complexes Chem. Biol.* **1994**, 119.
- (16) Park, J. M.; Muhoberac, B. B.; Dubin, P. L.; Xia, J. *Macromolecules* **1992**, 25, 290.
- (17) Xia, J.; Dubin, P. L.; Kim, Y.; Muhoberac, B. B.; Klimkowski, V. J. *J. Phys. Chem.* **1993**, 97, 4528.
- (18) Xia, J.; Dubin, P. L.; Dautzenberg, H. *Langmuir* **1993**, 9, 2015.
- (19) Xia, J.; Dubin, P. L.; Ahmed, L. S.; Kokufuta, E. in *Macro-Ion Characterization: From Dilute Solutions to Complex Fluids*; Schmitz, K. S., Ed.; ACS Symposium Series 548; American Chemical Society: Washington, DC, 1994; p 225.
- (20) Xia, J.; Dubin, P. L. *J. Chromatography A* **1994**, 667, 311.
- (21) Ahmed, L. S.; Xia, J.; Dubin, P. L. *J. Macromol. Sci., Pure Appl. Chem.* **1994**, A31 (1), 17.
- (22) Petit, F.; Audebert, R.; Iliopoulos, I. *Colloid Polym. Sci.* **1995**, 273, 777.
- (23) Tan, J. S.; Harrison, C. A.; Li, J.-T.; Caldwell, K. To be submitted for publication.
- (24) Unpublished results.
- (25) Whitesides, T. H. Private communication.
- (26) Rose, P. I. In *The Theory of the Photographic Process*, 4th ed.; James, T. H., Ed.; Macmillan Publishing Co., Inc.: New York, 1977; Chapter 2, p 51.
- (27) Pezron, I.; Djabourov, M.; Leblond, J. *Polym. Sci., Part B: Polym. Phys.* **1991**, 32, 3201.
- (28) Takahashi, A.; Kato, T.; Nagasawa, M. *J. Phys. Chem.* **1967**, 71, 2001.
- (29) Fisher, L. W.; Sochor, A. R.; Tan, J. S. *Macromolecules* **1977**, 10, 949.
- (30) Li, Y.; Dubin, P. L.; Dautzenberg, H.; Luck, U.; Hartmann, J.; Tuzar, Z. *Macromolecules* **1995**, 28, 6795.
- (31) Rose, P. I. In *Encyclopedia Polymer Science and Engineering*, 2nd ed.; John Wiley & Sons: New York, 1987; Vol. 7, p 502.
- (32) Dobrynin, A. V.; Colby, R. H.; Rubinstein, M. *Macromolecules* **1995**, 28, 1859.
- (33) Eisenberg, H.; Woodside, D. J. *Chem. Phys.* **1962**, 36, 1844.
- (34) Akcasu, A. Z.; Han, C. C. *Macromolecules* **1979**, 12, 276.
- (35) Burchard, W. *Adv. Polym. Sci.* **1983**, 48, 75.
- (36) McQuarrie, D. A. *Statistical Mechanics*; Harper & Row Publishers: New York, 1976; p 333.
- (37) Dobrynin, A. V.; Rubinstein, M.; Joanny, J. F. *Macromolecules*, in press.

MA961915U